Uroguanylin Increases Ca2+ Concentration in Astrocytes via Guanylate Cyclase C-independent Signalling Pathway

Nikola Habek
Sveuciliste u Zagrebu Medicinski fakultet
Martina Ratko
Sveuciliste u Zagrebu Medicinski fakultet
Aleksandra Dugandžić (aleksandra.dugandzic@mef.hr)
Croatian Institute for Brain Research, University of Zagreb, Zagreb, Croatia https://orcid.org/0000-0001-9454-7207

Research article

Keywords: electrophysiology, primary culture, brain slices, intracellular Ca2+ and pH, hanging wire test, Rota-rod test

Posted Date: September 22nd, 2020

DOI: https://doi.org/10.21203/rs.3.rs-52912/v1

Abstract

Background: Guanylin peptides (GPs), guanylin and uroguanylin (UGN), are intestinal peptides which activate guanylate cyclase C (GC-C) and increase cGMP concentration. In the brain, GC-C is located in the midbrain where GPs neuromodulate neuron activity. GC-C has also been reported in the hypothalamus where it plays an important role in the regulation of feeding and satiety. The existence of cGMP/GC-C independent signalling pathway for GPs was suggested two decades ago; however, the exact nature of the signalling pathway has not been discovered. Therefore, the aim of this study is to investigate the cGMP/GC-C independent signalling pathway in astrocytes which are a suitable model because they do not express GC-C.

Results: In this study, we performed patch clamp and intracellular Ca^{2+} concentrations and pH measurements in primary cultures of astrocytes and brain slices of WT, UGN KO, and GC-C KO mice. The function of GC-C independent signalling pathway in cerebellum was determined by behaviour tests in UGN and GC-C KO mice. We showed, for the first time, that UGN induces changes in intracellular Ca^{2+} levels in different mouse brain regions. In addition to midbrain and hypothalamus, GC-C is also expressed in cerebral and cerebellar cortex. Presence of two signalling pathways in the cerebellum (UGN hyperpolarized Purkinje cells via GC-C and increased intracellular Ca^{2+} concentration in astrocytes) lead to a difference in motoric function in GC-C KO and UGN KO mice probably via difference in regulation of intracellular pH in astrocytes.

Conclusion: The results of this study suggest that the effects of UGN on astrocytes via a Ca^{2+}- dependent signalling pathway could be involved in the modulation of neuronal activity.

Background

Guanylin peptides (GPs) belong to the family of natriuretic peptides which includes: guanylin (GN), uroguanylin (UGN), lymphoguanylin, and the recently discovered renoguanylin. After a meal, GN and UGN are secreted in the gut lumen and in the blood [1–3]. GPs activate guanylate cyclase C (GC-C) which leads to an increase in the intracellular concentration of cyclic guanosine monophosphate (cGMP), followed by activation of cGMP-dependent protein kinase G (PKG). In the intestine, GC-C is described as a receptor for the heat-stable enterotoxin of *Escherichia coli* (ST-a) [4], whose strong activation leads to diarrhoea. When GC-C was also discovered in extra-intestinal tissues which are not exposed to STa, like kidneys, reproductive system, brain and lungs [5, 6], the existence of endogenous activators of GC-C were assumed. In 1992 Currie et al isolated GN from rat intestine, and a year later Hamra et al (1993) isolated UGN from opossum urine [7, 8].

In the brain, natriuretic peptides play an important role in neuronal differentiation, neuromodulation and neuroprotection. The role of GC-C and GPs in the brain are still a mystery. GC-C is reported in midbrain dopaminergic neurons of substantia nigra compacta and the ventral tegmental area. Its activation increases the firing frequency induced by metabotropic glutamate (mGluR) and muscarinic acetylcholine

receptors (mAChR). Therefore, GC-C knockout (KO) animals develop ADHD-like behaviour with increased locomotor activity and seeking behaviour [9]. Furthermore, GC-C is expressed in pro-opiomelanocortin (POMC)-expressing neurons of the Arcuate nucleus of hypothalamus where it changes feeding behaviour, activity of brown adipose tissue, and energy balance. Therefore, GC-C and UGN KO mice have increased body weight [10, 11]. Intranasal application of UGN leads to an increase in BAT activity followed by a decrease in blood glucose concentration [12]. Prolonged application of UGN in brain ventricles leads to a decrease in body weight and development of brown adipose tissue via the sympathetic nervous system. Recent publications suggest the important role of brain UGN in metabolic regulation and possible involvement in the development of metabolic syndrome [11, 13].

The existence of the cGMP/GC-C independent signalling pathway was suggested two decades ago. Binding sites for STa in the intestine are not completely co-localized with the expression of GC-C. Therefore, in the intestine there exist two types of binding sites for STa. First is GC-C which has a low affinity binding site [14]. The other one is GC-C-independent and has a high affinity binding site, which constitutes 10% of all STa binding sites. This additional signalling pathway is still present in GC-C KO mice and its activation leads to an increase in intracellular Ca^{2+} concentrations [15]. In 1993 Mann et al showed the existence of the GC-C independent signalling pathway for STa in cultured rat small intestine epithelial cells (IEC-6). They only concluded that this novel signalling pathway is cGMP-independent with no suggestions which other signalling pathways could be involved [16]. Since GPs are natriuretic peptides it is not surprising that UGN KO animals have increased blood pressure [17]. Hypertension likely develops because there is no activation of the GC-C-independent signalling pathway in the kidney where this pathway has been predominantly investigated [18–21].

The existence of the GC-C-independent signalling pathway for GPs has been suggested and the search for a new signalling pathway has lasted for decades. Here, we report that GC-C is not the only existing receptor for GPs in the brain and the brain GC-C is not only present in the midbrain and hypothalamus.

Results

Uroguanylin increases intracellular Ca^{2+} concentration in different brain regions

We performed Ca^{2+} imaging in different regions on brain slices of adult wild-type (WT) mice and GC-C and UGN knockout (KO) mice to investigate the possible differences in presents of GC-C independent signalling pathway. In cerebellar cortex, UGN (100 nM) increased intracellular Ca^{2+} concentrations in cells in both, molecular and granular layers in WT and GC-C KO animals (Fig. 1a left). Bradykinin (BK, 1 μM) was used as positive control (Fig. 1a right) [22]. In cerebral cortex UGN (100 nM) (Fig. 1b left) and BK (1 μM) (Fig. 1b right) increased intracellular Ca^{2+} concentrations in both WT and GC-C KO animals. Increase in Ca^{2+} concentrations upon both hormones lasted a bit longer in WT compared to GC-C KO mice in cerebral cortex.

Expression of guanylate cyclase C in the brain

As published recently, GC-C is expressed in POMC neurons of hypothalamic arcuate nucleus [12]. To determine which cells express GC-C in other brain regions, we performed co-localization experiments with specific astrocyte marker Gliar Fibrillary Acidic Protein (GFAP) and specific neuronal marker Neuronal Nuclei marker (NeuN). GC-C was not found in astrocytes because it is not co-localized with GFAP. GC-C is expressed on cell membranes of the neurons in the hypothalamus (Fig. 2a), cerebellar Purkinje cells (Fig. 2b), neurons of cerebellar deep nuclei (Fig. 2c) and cerebral cortex (Fig. 2d) as previously shown in human prefrontal cortex [23]. GC-C KO animals were used as negative control.

Function of signalling pathways for uroguanylin in the cerebellum

The physiological importance of GC-C expressed in midbrain and hypothalamus has been investigated. In this part of the study we would like to investigate potential effects of GC-C and Ca^{2+} signalling pathway in the function of cerebellum. Purkinje cells express GC-C (Fig. 2b), therefore it is not surprising that hyperpolarization of those cells due to UGN (100 nM - Fig. 3a - original trace) was not present in GC-C KO animals (WT: -7.2 ± 1.4 mV, n = 5; GC-C KO: 1.6 ± 1.7 mV, n = 4, t-test: t(7) = 4.074, p = 0.0047) (Fig. 3b). There is no difference in starting potential of Purkinje cells of WT and GC-C KO mice (WT: -39.2 ± 2.1 mV, n = 17; GC-C KO: -39.9 ± 1.8 mV, n = 10, t-test: t(25) = 0.2065, p = 0.8381). UGN effects were in positive correlation (r = 0.83) to starting membrane potentials (Fig. 3b). Due to hyperpolarizing effects, UGN significantly decreased the rate of spontaneous action potentials in Purkinje cells (Control: 15.8 ± 0.8 Hz; UGN (100 nM): 11.6 ± 1.7 Hz, n = 8, t(14) = 2.224, p = 0.0431). Since the activation of GC-C does not involve changes in intracellular Ca^{2+} concentrations, UGN (100 nM) did not increase the intracellular Ca^{2+} concentration of Purkinje cells (Fig. 3c). Increased K^{+} concentrations were used as positive control and increase in Ca^{2+} concentrations due to hyperkalaemia (Fig. 3c - upper panel) corresponds to occurrence of action potentials (Fig. 3c - lower panel).

In cerebellum exist two signalling pathways for UGN, GC-C dependent on Purkinje cells and Ca^{2+} dependent in other cell types, like astrocytes. To determine the possible effects of both signalling pathways on balance and strength, we performed behaviour tests on GC-C KO and UGN KO animals. The difference between those animals is that in GC-C KO mice the UGN can activate Ca^{2+} signalling pathway, while in UGN KO the both signalling pathways for UGN are inactivated. Accelerating speed rota-rod test showed that GC-C KO animals stayed on the rod shorter that UGN KO mice (GC-C WT: 151 ± 21 s ; GC-C KO: 91 ± 14 s; UGN WT: 141 ± 23 s UGN KO 200 ± 11 s, n = 6, mean ± SEM, ANOVA: F(3,20) = 6.23059, p = 0. 0037) and reached maximal speed of the rod 15.2 ± 1.6 rpm which is significantly lower to UGN KO animals (27.8 ± 1.4 rpm, mean ± SEM, t-test: t(10) = 6.001, p = 0.0001) (Fig. 4). When the test was repeated GC-C KO showed no difference to GC-C WT littermates but in all trials, they performed significantly worse compared to UGN KO mice. UGN KO mice in 3rd and 4th trial become significantly better compared to WT littermates (UGN WT) (2nd trial: GC-C WT: 151 ± 14 s ; GC-C KO: 112 ± 21 s; UGN WT: 133 ± 35 s UGN KO 200 ± 17 s, n = 6, ANOVA: F(3,20) = 2.61318, p = 0. 07953, 3rd trial: GC-C WT: 146 ± 15 s ; GC-C KO: 108 ±

11 s; UGN WT: 136 ± 30 s UGN KO 236 ± 15 s, n = 6, mean ± SEM, ANOVA: F(3,20) = 8,50209, p = 0,000771; 4th trial: GC-C WT: 167 ± 17 s ; GC-C KO: 124 ± 15 s; UGN WT: 136 ± 22 s UGN KO 239 ± 21 s, n = 6, mean ± SEM, ANOVA: F(3,20) = 7.21935, p = 0. 00181). The similar results were shown for hanging wire test where GC-C KO mice scored significantly fewer points compared to UGN KO mice which 4 of 6 mice scored maximal 15 points (GC-C WT: median [IQR] = 8 [5.25]; GC-C KO: median [IQR] = 3 [3.75]; UGN WT: median [IQR] = 6 [7.75]; UGN KO: median [IQR] = 15 [4.5], n = 6, Kruskal-Walls test with post-hoc Dunn test, p = 0.0182).

Uroguanylin activates GC-C-independent but Ca^{2+}-dependent signalling pathway in astrocytes

Accordingly to GC-C protein expression, at mRNA level, GC-C was found in the cerebral cortex, cerebellum, hypothalamus, and midbrain but not in isolated astrocytes (Fig. 5a, original gel is shown in Additional file 2). Since the Ca^{2+} response to UGN still exists but lasting a little bit shorter in cerebral cortex of GC-C KO animals, we examined the Ca^{2+} response upon UGN (100 nM) in Sulforhodamine 101 (SR101) positive cells (marker for astrocytes) in cerebral cortex of GC-C KO and UGN KO mice and their WT littermates. Results are presented as a ratio to starting values. There was no difference in astrocytes Ca^{2+} response to UGN in GC-C KO and UGN KO mice when compared it to their WT littermates (GC-C WT and UGN WT, Fig. 5b). In addition, some SR101 negative cells showed no increase in intracellular Ca^{2+} concentration upon UGN stimulation similarly as shown above for cerebellar Purkinje cells (Fig. 5c).

To better characterised UGN Ca^{2+} signalling pathway, we used primary culture of astrocytes. GN and UGN (10 nM, each) hyperpolarized astrocytes (-4.5 ± 0.6 mV and − 4.0 ± 1.5 mV, n = 3, respectively) (Fig. 6a - the original trace, Fig. 6b - summarized data). Those effects were in negative correlation (r = -0.92, p = 0.0092) to starting membrane potential (Fig. 6c). During the paired experiments, membrane permeable cGMP (8 Br cGMP, 100 μM) depolarized the same cells (2.2 ± 0.4 mV, n = 3) (Fig. 6a - the original trace, Fig. 6b - summarized data).

Since the cGMP is not a second messenger for GPs in astrocytes, to confirm existence of Ca^{2+} signalling pathway, we performed Ca^{2+} imaging and showed that UGN (100 nM) leads to an increase in intracellular Ca^{2+} concentration in those cells (Fig. 6d). BK (1 μM), used as positive control, showed significantly smaller effects [22].

Uroguanylin changes transport of H^+ and bicarbonate

Possible physiological importance of this novel signalling pathway is the regulation of different membrane transporters. We examined the effect of UGN (100 nM) on astrocyte pH_i. UGN application increased pH_i recovery slope after ammonia pulse by 70% due to an increase of Na^+/H^+ exchanger (NHE) activity (t-test: t(7) = 2.429, p = 0.0455) (Fig. 7a – original trace, Fig. 7c - summarized). Furthermore, UGN (100 nM) increased the slope of cell alkalization after astrocyte exposure to CO_2/HCO_3^- by 2.5 times (t-

test: t(5) = 2.711, p = 0.0422), suggesting an activation of HCO_3^- transport by UGN (Fig. 7b – original trace, Fig. 7c - summarized).

Discussion

For natriuretic peptides, like atrial natriuretic peptide, in addition to guanylate cyclase receptor, another receptor exists. Activation of this additional signalling pathway leads to an increase in intracellular Ca^{2+} and cAMP concentrations [24]. In the cell culture of human proximal kidney cells, GC-C independent signalling pathway for guanylin peptides involves an activation of pertussis toxin sensitive G protein coupled receptor [19]. The physiological importance and existence in the brain of this cGMP-independent but Ca^{2+}-dependent signalling pathway for GPs has not been investigated.

First, we performed Ca^{2+} imaging experiments on brain slices of WT and GC-C KO mice in different brain regions. In cerebral cortex, but not cerebellar cortex, UGN effects lasted significantly shorter in GC-C KO mice then in WT animals. The effects of GC-C on Ca^{2+} signalling could be explained that some brain cells (like neurons) could express both signalling pathways for UGN. Difference in Ca^{2+} response to UGN in GC-C KO and WT mice were abolished when we examined the SR101 positive cells (astrocytes) in cerebral cortex in GC-C KO and their WT littermates which support the hypothesis. In cerebellar cortex, UGN did not change intracellular Ca^{2+} concentrations of Purkinje cells. Since the GC-C is present in the cerebral cortex and cerebellum in addition to previously known expression in hypothalamus and midbrain, it is not surprising that UGN hyperpolarized Purkinje cells which express GC-C in WT but not GC-C KO animals. Due to hyperpolarization, the rate of spontaneous action potentials is decreased. However, missing only GC-C in GC-C KO mice did not change significantly their performance in behaviour tests. In other hand, where there is no activation of both GC-C and Ca^{2+} signalling pathway, UGN KO mice performed much better than GC-C KO and UGN WT littermates. To better understand the negative effects of UGN via Ca^{2+} signalling pathway we performed experiments in primary culture of astrocytes. UGN decrease extracellular pH via increasing NHE activity and removal of bicarbonate from the extracellular fluid. Therefore, we can hypothesize that extracellular alkalinisation due to lack of UGN effects on astrocytes in UGN KO mice will increase neuronal activity which could explain their better performance during behaviour tests (discussed more later).

Since the GC-C is not expressed in astrocytes, they are a good model for further study of GC-C independent signalling pathway for guanylin peptides. GPs changed membrane potential of primary astrocyte culture, showing the existence of GC-C/cGMP-independent signalling pathway. GPs could hyperpolarized astrocytes via an increase of Cl^- or K^+ conductance since the effects of GPs are in negative correlation to the starting membrane potential (less negative membrane potential leads to higher hyperpolarization). We showed that UGN leads to an increase in intracellular Ca^{2+} concentration which could activate Ca^{2+}-dependent Cl^- channels or calcium-regulated K^+ channels (see Additional file 2) [25–27]. In contrast to effects of GPs, membrane permeable cGMP depolarized the same cells probably via an inhibition of K^+ conductance, as previously shown [19–21, 28].

Changes in H^+ and HCO_3^- transport will change intracellular pH (pH_i) and pH of brain extracellular fluid (pH_e). Since H^+ inhibits N-methyl-D-aspartate (NMDA) glutamate receptors and voltage-gated Ca^{2+} channels, an alkalinisation or acidification of pH_e can increase or decrease neuronal activity [29, 30]. It is known that cGMP decreases astrocyte pH_i by inhibition of NHE [31]. In other cell models, UGN inhibits H^+ transport (NHE, H^+-ATP-ase) via cGMP [32, 33] and changing the expression of Cl^-/HCO_3^- exchanger (Slc26a4) [34]. Since we established that cGMP is not a second messenger for UGN in astrocytes, the regulation of H^+ and HCO_3^- transport via Ca^{2+}-signalling pathway could be regulated differently [35]. Indeed, UGN application increased the pH_i recovery slope after the ammonia pulse by increasing the activity of NHE and increased slope of cell alkalization after astrocyte exposure to CO_2/HCO_3^- suggesting activation of HCO_3^- transport. It is known that NHE and HCO_3^- transporters are involved in the pathophysiology of ischemic injury; however, further research is needed to define the possible involvement of UGN in development of brain ischemic injury [36–38].

Conclusions

The presented results suggest a neurophysiological importance of GC-C independent signalling pathway for UGN in astrocytes. In neurons of substantia nigra compacta and ventral tegmental area, UGN via GC-C potentiates the excitatory responses induced by glutamate via mGluR type 1 and 5 and acetylcholine via mAChR, as described previously [9]. Our study suggests different effects of UGN on neurons in different brain regions since UGN changes membrane potential and decreases spontaneous action potential rate of cerebellar Purkinje cells. In addition to GC-C-dependent signalling pathway in neurons, in astrocytes, UGN binds to GC-C-independent receptors whose activation leads to an increase in intracellular Ca^{2+} concentration. The effects of UGN via a novel GC-C-independent signalling pathway in astrocytes regulates intracellular and extracellular pH by increased activity of NHE and HCO_3^- transport (see Additional file 2).

Methods

Animals

Animals used in this study were male WT mice of C57Bl/6 strain. GC-C and UGN KO mice that were generated (C57Bl/6 background) as described previously [10, 39]. GC-C and UGN KO mice were generously donated by Kris A. Steinbrecher, PhD and prof Anjaparavanda P Naren, PhD (Cincinnati Children's Hospital Medical Center, Cincinnati, Ohio, USA). Before experiments were performed animals were maintained for several generations in our animal facility. Experiments were carried on 4–6 months old male mice and primary astrocyte cultures were isolated from new-borns (postnatal day 0) of WT animals.

We minimized animal suffering and reduced the number of animals used by using WT and GC-C KO littermates only when necessary. Mice were fed with standard rodent chow and had water and food *ad libitum* with day/night cycles of 12 h at 23^{O}C and humidity between 50–75%.

WT and GC-C KO mice were anaesthetized with intraperitoneal injections of 2, 2, 2 – Tribromoethanol (250 mg/kg, Sigma-Aldrich, St. Luis, MO, USA) (IACUC Guidelines: Anaesthesia) and transcardially perfused with oxygenated (95% O_2/5% CO_2) ice-cold N-Methyl-D-Glucamine (NMDG) aCSF containing: 93 mM NMDG, 93 mM HCl, 2.5 mM KCl, 1.2 mM NaH_2PO_4, 30 mM $NaHCO_3$, 20 mM HEPES, 10 mM $MgSO_4$, 0.5 mM $CaCl_2$ and 25 mM glucose, as described previously [40]. The brain was quickly isolated and cut slices for electrophysiological and Ca^{2+} measurements.

Primary astrocyte culture isolation by magnetic activated cell separation

WT mice pups (postnatal day 0) were anaesthetized on ice which is consider an IACUC Standard Procedure and decapitated when animal skin becomes light blue. Brains were carefully removed, meninges were stripped off, and brains were placed in StemPro® Accutase® (Thermo Fisher Scientific, Waltham, MA, USA) enzyme solution for 60 min on room temperature (RT). The enzyme reaction was stopped with the same volume of Dulbecco's Modified Eagle's Medium/F12 (DMEM/F12) (Thermo Fisher Scientific). Supernatant-containing cells were collected and centrifuged for 6 min at 300 g. Supernatant solution was removed and a cell pellet was subjected to magnetic activated cell separation (MACS) as described previously [41].

The cell pellet was incubated with Anti-Glast-biotin (Milteny Biotec, Bergisch Gladbach, Germany) antibody in 0.01 M phosphate buffer saline (PBS) containing 0.5% bovine serum albumin (BSA) for 15 min at + 4 ^{O}C. Cells were washed with PBS/0.5% BSA, centrifuged 10 min on 300 g and incubated with anti-biotin Microbeads antibody (Milteny Biotec) in PBS/0.5% BSA for 15 min at + 4 ^{O}C. Cells were then washed with PBS/0.5% BSA, centrifuged for 10 min at 300 g, a supernatant was removed, and cells were re-suspended in PBS/0.5% BSA. Columns for MACS were prepared and placed in a strong magnetic field (Milteny Biotec). The cell suspension was passed through the MACS column where astrocytes, tagged with anti-Glast/biotin/microbeads, were bound to column due to the magnetic field. The column was washed with PBS/0.5% BSA 3 times. Finally, the column was removed from the strong magnetic field and the remaining cells, which comprise 99% of astrocytes, were collected and plated on coverslips. Astrocytes were cultured in DMEM/F12 with an addition of 10% Foetal Calf Serum, 100 U/mL penicillin, and 100 µg/mL streptomycin, and maintained in an atmosphere of 5% CO_2/95% air at 37 °C. Cells were used 3–10 (6.9 ± 0.5, mean ± SEM, n = 12) 6 days after isolation. For RNA isolation, astrocytes were re-suspended in TRI Reagent® Solution (Thermo Fisher Scientific).

RT-PCR

Total RNA was isolated from primary astrocytes, brain regions, and intestines of WT mice by TRI Reagent® Solution (Thermo Fisher Scientific). Mice were sacrificed by cervical dislocation followed by isolation of brain and intestine. Cerebral cortex, cerebellum, hypothalamus, and midbrain were carefully dissected from the brain. Total RNA (1 µg) from cells or tissues was used for cDNA synthesis (GoScript Reverse Transcription System (Promega, Madison, WI, USA)). PCR was performed using cDNA (1 µL) and the following primer sets: GC-C S: 5' TGCGCTGCTGGTGTTGTGG 3', AS: 5' CCCGAGGCCTGTCTTTTCTGTAA 3' (product size 341 bp); GAPDH S: 5' ACGGCCGCATCTTCTTGTG 3'; AS: 5' CCCATTCTCGGCCTTGACTG 3' (product size 235 bp), in the following conditions: 2 min at 94 °C, 30 s at 58.8 °C, 1 min at 72 °C (1 cycle); 30 s at 94 °C, 30 s at 58.8 °C, 1 min at 72 °C (30 cycles). The primer set for GC-C was designed to give equal product size for both GC-C isoforms. PCR products were analysed by agarose gel electrophoresis. GAPDH expression was used as cDNA control and a negative control was without cDNA in the reaction mixture. PCR products were verified by sequencing.

Immunohistochemistry

WT and GC-C KO mice were anaesthetized as described above and transcardially perfused with PBS and 4% paraformaldehyde (PFA). Brains were isolated and put in 4% PFA for 24 h and cryoprotected in 20% and 30% sucrose in PBS. 4 µm slices were cut on cryostat Leica CM3000.

After rehydration in PBS and antigen retrieval (5 min in boiling 10 mM Citrate buffer, pH = 6), permeabilization in 0.2% Tween-20 in PBS for 8 min was performed. Sections were blocked 1 h at RT with 1% BSA in PBS and incubated with primary antibody against GC-C (1:25, Santa Cruz, Santa Cruz, USA, sc-34428) at + 4 ^{o}C. After 3 washes with PBS, sections were incubated in secondary antibody (1:500, Alexa fluor 488, Thermo Fisher Scientific) for 1 h at RT. After washing, sections were incubated overnight with another primary antibody, anti-NeuN (1:1000, Abcam plc., Cambridge, UK, ab104225) or anti-GFAP (1:1000, DAKO, Agilent Technologies, Santa Clara, CA, USA, Z 0334) at + 4 ^{o}C. After 3 washes for 10 min in PBS, sections were incubated with secondary antibody (1:200, Cy5, Jackson ImmunoResearch Laboratories, Inc., West Grove, PA, USA, code: 711-175-152) for 1 h at RT. After washing, sections were mounted by fluorescent mounting medium (DAKO).

Fluorescent signals were acquired by Zeiss LSM 510-META confocal microscope. Alexa flour 488 was excited by 488 nm argon laser line and fluorescent emission was collected from 505–530 nm. Cy5 labelling NeuN or GFAP was excited by 633 nm HeNe laser line and fluorescent signal was collected from 650–680 nm.

Electrophysiology

Coverslips with astrocytes were placed in the recording chamber and perfused with artificial cerebrospinal fluid (aCSF) without HCO_3^- (aCSF – HCO_3^- free) containing: 154 mM NaCl, 1.25 mM NaH_2PO_4, 2 mM $MgCl_2$, 3 mM KCl, 2 mM $CaCl_2$ and 10 mM glucose. Patch pipettes (5–7 MΩ) were filled with an internal solution containing: 115 mM K-gluconate, 20 mM KCl, 1.5 mM $MgCl_2$, 10 mM phosphocreatine, 10 mM HEPES, 2 mM Mg-ATP and 0.5 mM GTP. Freshly made Nystatin (160 µM) was added to the internal

solution to permeabilize cell membrane. The starting resistance of prepared pipettes was 5.3 ± 0.3 MΩ, n = 4, mean ± SEM and the liquid junction potential was compensated before the establishment of the cell-attached mode in all recordings. Cells were visualized under upright microscope Axioskop 2 FS plus (Zeiss, Oberkochen, Germany) and membrane potentials were recorded in perforated whole-cell configuration by SEC 0.5LX npi (npi electronic GmbH, Tamm, Germany) amplifier and WinEDR software (University of Strathclyde, Glasgow, UK).

For electrophysiological and Ca^{2+} measurements on brain slices, WT and GC-C KO mice were anaesthetized as described above and transcardially perfused with oxygenated (95% O_2/5% CO_2) ice-cold N-Methyl-D-Glucamine (NMDG) aCSF. The brain was quickly isolated and cut in 300 µm thick slices (Vibratome 1000 plus, The Vibratome Company, St. Louis, MO, SAD) in ice-cold NMDG-aCSF. Initial recovery was done in the same solution at 32 ^{o}C for 10 min followed by additional recovery for at least 60 min at RT in oxygenated aCSF: 128 mM NaCl, 1.25 mM NaH_2PO_4, 26 mM $NaHCO_3$, 2 mM $MgSO_4$, 3 mM KCl, 2 mM $CaCl_2$, and 10 mM glucose before use.

Cerebellar slices of WT and GC-C KO mice were placed in the recording chamber and perfused (2–3 mL/min at 33 ± 1 ^{O}C) with oxygenized aCSF: 127 mM NaCl, 10 mM D-glucose, 1.25 mM NaH_2PO_4, 26 mM $NaHCO_3$, 1 mM $MgCl_2$, 3 mM KCl and 2 mM $CaCl_2$. Purkinje cells were identified as large cells between the granular and molecular layers of cerebellar cortex under DIC. We used the same internal solution as described before; the size of patch clamp pipette was 6.0 ± 0.6 MΩ, n = 13, mean ± SEM. After establishing a seal, the cell membrane was mechanically ruptured.

Ca^{2+} Imaging

Astrocytes were incubated with 10 µM Fluo-4 AM in Hanks' Balanced Salt Solution (HBSS) (Sigma-Aldrich) on 37 ^{o}C in 5% CO_2/95% air for 15 min and washed with HBSS before imaging.

Brain slices were loaded with 0.5 µM of SR101 (when applied) and 10 µM of Fluo-4 AM dye (Thermo Fisher Scientific) [42] or Oregon Green 488 BAPTA-1 AM (Thermo Fisher Scientific) in oxygenated aCSF containing 100 mM of mannitol for 20 min and recovered for 10 min in oxygenated aCSF at RT. Between two and three brain slices for each imaged region per animal were used.

The imaging was done using a Zeiss LSM 510 META confocal microscope. Slices or cells on coverslips were placed in the recording chamber and excited using 488 nm argon laser line and fluorescent emission was collected above 520 nm. The SR101 was excited using 543 nm HeNe laser line and fluorescent emission was collected above 560 nm. Acquired rate was 1 Hz. Analysis of fluorescent signal intensity was performed in MATLAB (MathWorks, Natick, MA, USA) and presented as $\Delta F/F_0$. The Ca^{2+} response in astrocytes were determine by measuring only the SR101 positive cells.

pH measurements

Astrocytes on coverslips were loaded with 10 μM BCECF, AM (Thermo Fisher Scientific) in HBSS for 15 min in 5% CO_2/95% air at 37 °C and washed before imaging. Coverslips were put in the recording chamber and placed on inverted microscope Axiovert 10 (Zeiss). Cells were excited with two fluorescent wavelengths at 436 and 488 nm and emissions were detected at 520–560 nm with a single-photon-counting tube (H3460-04; Hamamatsu, Herrsching, Germany). Results were collected, analysed by Biofluor software, and presented as fluorescence ratio 488/436 nm.

An activity of NHE was tested by ammonia pulse [43]. Cells mounted on the recording chamber were perfused with aCSF – HCO_3^- free. After initial recording, 20 mM NH_4Cl was added. During an ammonia pulse, NH_3 enter the cells and binds H^+ ions leading to alkalization. After removal, NH_3 cells acidify and Na^+/H^+ exchanger returns pH to normal values by H^+ transport (schematic representation Fig. 7a).

HCO_3^- transport was tested after initial perfusion of cells with aCSF – HCO_3^- free followed by perfusion with saturated aCSF (containing 26 mM $NaHCO_3$) with 5% CO_2/95% O_2. Cell alkalinisation occurred due to HCO_3^- transport.

Behaviour tests

Hanging Wire Test was performed as previously described [44]. Animals grabbed the middle of 38 cm long and the 2 mm thick wire fixed at the height of 49 cm. The latency until animal fell down was recorded. The maximum of 30 s was used and the following points were assigned: 1–5 s one point; 6–10 s two points; 11–20 s three points; 21–30 s four points; more than 30 s or when mice reached the end of wire five points. If the recorded time was less than 5 s which could happen when animals did not hold on the wire properly, the experiment was repeated 3 times to get a better score. For all animals which scored 5 points at 2 mm wire (easy), the experiment was repeated using 4 mm wire (intermediate). Again, animals scored maximal 5 pints continued with the experiment using 6 mm wire (hard). All points were finally added. The maximal score was 15.

Rota-rod test was performed using Rota-Rod Model57604 with a rod of 3 cm diameter (Ugo Basile SRL, Gemonio, Italy) [45]. After the training period of 30 s at 5 rpm, the rod was accelerated from 5 to 40 rpm over 5 min. The endpoint was defined as the time when a mouse fell from the rod or was not able to walk on rotating rod. The first experiment was test one, which was followed by 3 trials in two consecutive days with the resting time for at least 6 h.

Statistical Analyses

For electrophysiological, Ca^{2+}, and pH experiments as minimally required three animals per group were measured. For behaviour test, six animals per group were measured as previously shown [46]. The data are presented as median and interquartile range (IQR) or mean ± standard error of the mean (SEM). For statistical analyses Student's t-test was used, where each effect was compared with its own control. If more than two parameters were compared we used ANOVA with post-hoc Tukey test. Statistical analysis for hanging wire behaviour test was done by Kruskal-Walls test with post-hoc Dunn test. A p value 0.05

was considered significant and is indicated by an asterisk. For statistical analyses, the GraphPad Instat (GraphPad Software, San Diego, CA, USA) statistical software was used.

Abbreviations

aCSF: artificial cerebrospinal fluid; BK: bradykinin; BSA: bovine serum albumin; cGMP - cyclic guanosine monophosphate; DMEM/F12: Dulbecco's Modified Eagle's Medium/F12; GN - guanylin; GC-C - guanylate cyclase C; GC-C KO: GC-C knockout mice; GFAP: Gliar Fibrillary Acidic Protein; GP: Guanylin peptide; HBSS: Hanks' Balanced Salt Solution; mAChR: muscarinic acetylcholine receptors; MACS: magnetic activated cell separation; mGluR: metabotropic glutamate receptor; NHE: Na^+/H^+ exchanger; NeuN: Neuronal Nuclei; PBS: phosphate buffer saline; POMC: pro-opiomelanocortin; RT: room temperature; ST-a: heat-stable enterotoxin of Escherichia coli; SR101: Sulforhodamine 101; UGN - uroguanylin; UGN KO: UGN knockout mice; WT: wild-type

Declarations

Ethics approval and consent to participate:

All experiments were approved by the University of Zagreb, School of Medicine Ethics Committee. They were performed in an accordance with the Ethical Codex of Croatian Society for Laboratory Animal Science and the ARRIVE guidelines.

Consent for publication:

Not applicable

Availability of data and materials:

All data generated or analysed during this study are included in this published article [and its supplementary information files].

Competing interests:

The authors declare that they have no competing interests.

Funding:

This publication was co-financed by the European Union through the European Regional Development Fund, Operational Programme Competitiveness and Cohesion, grant Agreement No. KK.01.1.1.01.0007,

CoRE - Neuro. The work of doctoral student N.H. has been supported in part by the “Young researchers' career development project – training of doctoral students” of the Croatian Science Foundation funded by the European Union from the European Social Fund. This study is financed by the Croatian science foundation research grant (IP-2018-01-7416) and financially supported by the University of Zagreb.

Authors' contributions:

N.H. designed research, performed experiments, analysed data, statistical analysis, and wrote and revised the manuscript.

M.R. performed experiments and analysed data

A.D. designed research, collected and analysed data, wrote and revised the manuscript.

Acknowledgements:

We would like to thank Sandra Mavrić, Josip Dugandžić for expertise in graphic and video preparation. Especially we would like to thank Kris A. Steinbrecher, PhD and prof Anjaparavanda P Naren, PhD (Cincinnati Children's Hospital Medical Center, Cincinnati, Ohio, USA) for donating GC-C KO and UGN KO animals. We would also like to thank prof. Eberhard Schlatter (Experimental Nephrology, Department of Internal Medicine D, University Hospital Muenster, Muenster, Germany) for donating the set-up for micro-fluorescence measurements.

References

1. Carrithers SL, Jackson BA, Cai WY, Greenberg RN, Ott CE. Site-specific effects of dietary salt intake on guanylin and uroguanylin mRNA expression in rat intestine. Regul Pept. 2002;107(1-2):87-95.
2. Kita T, Kitamura K, Sakata J, Eto T. Marked increase of guanylin secretion in response to salt loading in the rat small intestine. Am J Physiol. 1999;277(5):G960-6.
3. Li Z, Knowles JW, Goyeau D, Prabhakar S, Short DB, Perkins AG, Goy MF. Low salt intake down-regulates the guanylin signaling pathway in rat distal colon. Gastroenterology. 1996;111(6):1714-21.
4. Schulz S, Green CK, Yuen PS, Garbers DL. Guanylyl cyclase is a heat-stable enterotoxin receptor. Cell. 1990;63(5):941-8.
5. Forte LR, Krause WJ, Freeman RH. Receptors and cGMP signalling mechanism for E. coli enterotoxin in opossum kidney. Am J Physiol. 1988;255(5 Pt 2):F1040-6.
6. Forte LR, Krause WJ, Freeman RH. Escherichia coli enterotoxin receptors: localization in opossum kidney, intestine, and testis. Am J Physiol. 1989;257(5 Pt 2):F874-81.
7. Currie MG, Fok KF, Kato J, Morre RJ, Hamra FK, Duffin KL, Smith CE. Guanylin: An endogenous activator of intestinal guanylate cyclase. Proc Natl Acad Sci USA. 1992;89(3):947-51.

8. Hamra FK, Forte LR, Eber SL, Pidhorodeckyj NV, Krause WJ, Freeman RH, et al. Uroguanylin: structure and activity of a second endogenous peptide that stimulates intestinal guanylate cyclase. Proc Natl Acad Sci USA. 1993;90(22):10464-8.
9. Gong R, Ding C, Hu J, Lu Y, Liu F, Mann E, et al. Role for the membrane receptor guanylyl cyclase-C in attention deficiency and hyperactive behavior. Science. 2011;333(6049):1642-6.
10. Begg DP, Steinbrecher KA, Mul JD, Chambers AP, Kohli R, Haller A, et al. Effect of guanylate cyclase-C activity on energy and glucose homeostasis. Diabetes. 2014;63(11):3798-804.
11. Valentino MA, Lin JE, Snook AE, Li P, Kim GW, Marszalowicz G, et al. A uroguanylin-GUCY2C endocrine axis regulates feeding in mice. J Clin Invest. 2011;121(9):3578-88.
12. Habek N, Dobrivojević Radmilović M, Kordić M, Ilić K, Grgić S, et al. Activation of brown adipose tissue in diet-induced thermogenesis is GC-C dependent. Pflug Arch. 2020;472(3):405-17.
13. Folgueira C, Beiroa D, Callon A, Al-Massadi O, Barja-Fernandez S, Senra A, et al. Uroguanylin action in the brain reduces weight gain in obese mice via different efferent autonomic pathways. Diabetes. 2016;65(2):421-32.
14. Crane MR, Hugues M, O'Hanley PD, Waldman SA. Identification of two affinity states of low affinity receptors for Escherichia coli heat-stable enterotoxin: correlation of occupation of lower affinity state with guanylate cyclase activation. Mol Pharmacol. 1992;41(6):1073–80.
15. Ganguly U, Chaudhury AG, Basu A, Sen PC. STa-induced translocation of protein kinase C from cytosol to membrane in rat enterocytes. FEMS Microbiol Lett. 2001;204(1):65–9.
16. Mann EA, Cohen MB, Giannella RA. Comparison of receptors for Escherichia coli heat-stable enterotoxin: novel receptor present in IEC-6 cells. Am J Physiol. 1993;264(1 Pt 1):G172-8.
17. Lorenz JN, Nieman M, Sabo J, Sanford LP, Hawkins JA, Elitsur N, et al. Uroguanylin knockout mice have increased blood pressure and impaired natriuretic response to enteral NaCl load. J Clin Invest. 2003;112(8):1244–54.
18. Carrithers SL, Ott CE, Hill MJ, Johnson BR, Cai W, Chang JJ, et al. Guanylin and uroguanylin induce natriuresis in mice lacking guanylyl cyclase-C receptor. Kidney Int. 2004;65(1):40-53.
19. Sindiće A, Başoglu C, Cerçi A, Hirsch JR, Potthast R, Kuhn M, et al. Guanylin, uroguanylin, and heat-stable euterotoxin activate guanylate cyclase C and/or a pertussis toxin-sensitive G protein in human proximal tubule cells. J Biol Chem. 2002; 277(20):17758-64.
20. Sindić A, Hirsch JR, Velic A, Piechota H, Schlatter E. Guanylin and uroguanylin regulate electrolyte transport in isolated human cortical collecting ducts. Kidney Int. 2005;67(4):1420-7.
21. Sindić A, Velic A, Başoglu C, Hirsch JR, Edemir B, Kuhn M, Schlatter E. Uroguanylin and guanylin regulate transport of mouse cortical collecting duct independent of guanylate cyclase C. Kidney Int. 2005;68(3):1008-17.
22. Dobrivojević M, Špiranec K, Gorup D, Erjavec I, Habek N, Radmilović M, et al. Urodilatin reverses the detrimental influence of bradykinin in acute ischemic stroke. Exp Neurol. 2016;284(Pt A):1-10.

23. Colantuoni C, Lipska BK, Ye T, Hyde TM, Tao R, Leek JT, et al. Temporal dynamics and genetic control of transcription in the human prefrontal cortex. Nature. 2011;478(7370):519-23.
24. Rose RA, Giles WR. Natriuretic peptide C receptor signalling in the heart and vasculature. J Physiol. 2008;586(2):353–66.
25. Agnel M, Vermat T, Culouscou JM. Identification of three novel members of the calcium-dependent chloride channel (CaCC) family predominantly expressed in the digestive tract and trachea. FEBS Lett. 1999;455(3):295–301.
26. Quandt FN, MacVicar BA. Calcium activated potassium channels in cultured astrocytes. Neuroscience. 1986;19(1):29-41.
27. Wilson CS, Mongin AA. The signaling role for chloride in the bidirectional communication between neurons and astrocytes. Neurosci Lett. 2019;689:33-44.
28. Wahler GM, Sperelakis N. Use of the cell-attached patch clamp technique to examine regulation of single cardiac K channels by cyclic GMP. Mol Cell Biochem. 1988;80(1-2):27-35.
29. DeVries SH. Exocytosed protons feedback to suppress the Ca^{2+} current in mammalian cone photoreceptors. Neuron. 2001;32(6):1107-17.
30. Traynelis SF, Cull-Candy SG. Proton inhibition of N-methyl-D-aspartate receptors in cerebellar neurons. Nature. 1990;345(6273):347-50.
31. Touyz RM, Picard S, Schiffrin EL, Deschepper CF. Cyclic GMP inhibits a pharmacologically distinct Na^+/H^+ exchanger variant in cultured rat astrocytes via an extracellular site of action. J Neurochem. 1997;68(4):1451-61.
32. da Silva Lima V, Crajoinas RO, Carraro-Lacroix LR, Godinho AN, Dias JL, Dariolli R, et al. Uroguanylin inhibits H-ATPase activity and surface expression in renal distal tubules by a PKG-dependent pathway. Am J Physiol. 2014;307(6):C532-41.
33. Lessa LM, Carraro-Lacroix LR, Crajoinas RO, Bezerra CN, Dariolli R, Girardi ACC, et al. Mechanisms underlying the inhibitory effects of uroguanylin on NHE3 transport activity in renal proximal tubule. Am J Physiol. 2012;303(10):F1399-408.
34. Rozenfeld J, Tal O, Kladnitsky O, Adler L, Efrati E, Carrithers SL, et al. The pendrin anion exchanger gene is transcriptionally regulated by uroguanylin: a novel enterorenal link. Am J Physiol. 2012;302(5):F614-24.
35. Costa-Pessoa JM, Figueiredo CF, Thieme K, Oliveira-Souza M. (2013) The regulation of NHE1 and NHE3 activity by angiotensin II is mediated by the activation of the angiotensin II type I receptor/phospholipase C/calcium/calmodulin pathway in distal nephron cells. Eur J Pharmacol. 2013;721(1-3):322-31.
36. Chesler M. Failure and function of intracellular pH regulation in acute hypoxic-ischemic injury of astrocytes. Glia. 2005;50(4):398-406.
37. Kintner DB, Su G, Lenart B, Ballard AJ, Meyer JW, Ng LL, Shull GE, Sun D. Increased tolerance to oxygen and glucose deprivation in astrocytes from Na(+)/H(+) exchanger isoform 1 null mice. Am J

Physiol. 2004;287(1):C12-21.

38. Yao H, Azad P, Zhao HW, Wang J, Poulsen O, Freitas BC, et al. The Na^+/HCO_3^- co-transporter is protective during ischemia in astrocytes. Neuroscience. 2016;339:329-37.
39. Mann EA, Jump ML, Wu J, Yee E, Giannella RA. Mice lacking the guanylyl cyclase C receptor are resistant to STa-induced intestinal secretion. Biochem Biophys Res Commun. 1997;239(2):463-6.
40. Zhao S, Ting JT, Atallah HE, Qiu L, Tan J, Gloss B, et al. Cell type–specific channelrhodopsin-2 transgenic mice for optogenetic dissection of neural circuitry function. Nat Methods. 2011;8(9):745-52.
41. Jungblut M, Tiveron MC, Barral S, Abrahamsen B, Knöbel S, Pennartz S, et al. Isolation and characterization of living primary astroglial cells using the new GLAST-specific monoclonal antibody ACSA-1. Glia. 2012;60(6):894-907.
42. Hirase H, Qian L, Barthó P, Buzsáki G. Calcium dynamics of cortical astrocytic networks in vivo. PLoS Biol. 2004;2(4):E96.
43. Bevensee MO, Weed RA, Boron WF. Intracellular pH regulation in cultured astrocytes from rat hippocampus. I. Role of HCO_3^-. J Gen Physiol. 1997;110(4):453-65.
44. Deacon RMJ. Measuring Motor Coordination in Mice. J Vis Exp. 2013; 29(75):e2609.
45. Paylor R, Nguyen M, Crawley JN, Patrick J, Beaudet A, Orr-Urtreger A. Alpha7 nicotinic receptor subunits are not necessary for hippocampal-dependent learning or sensorimotor gating: a behavioral characterization of Acra7-deficient mice. Learn Mem. 1998;5(4-5):302–16.
46. ChagnielL, Robitaille C, Lacharité-Mueller C, Bureau G, Cyr M. Partial dopamine depletion in MPTP-treated mice differentially altered motor skill learning and action control. Behav Brain Res.2012;228(1):9-15.

Figures

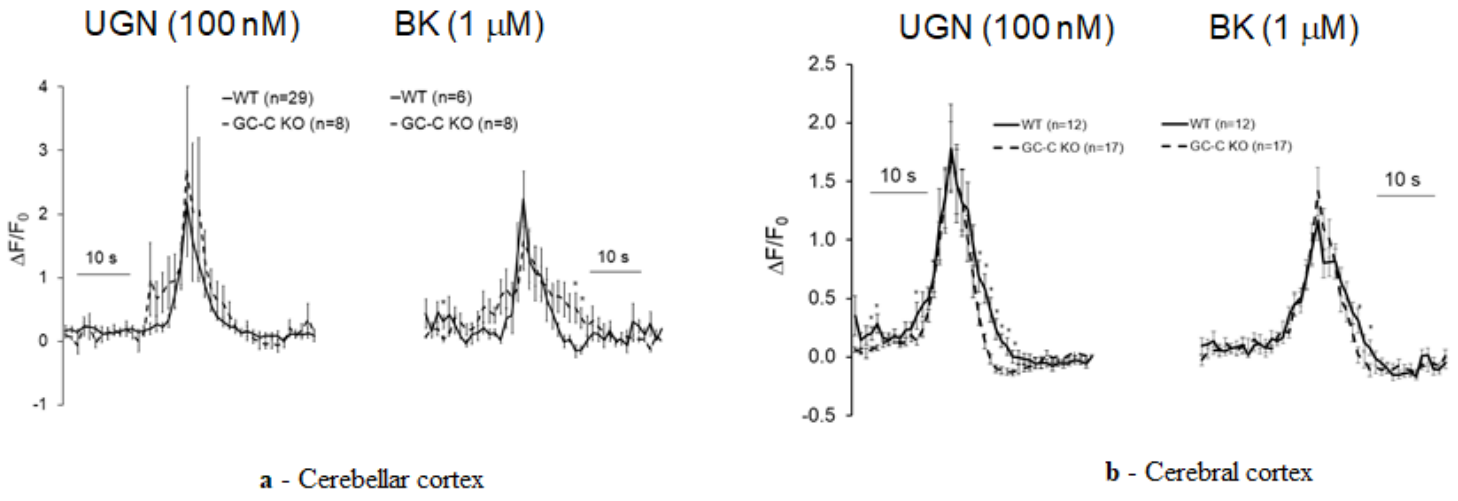

Figure 1

Uroguanylin (UGN) increases intracellular Ca2+ concentration in different brain regions. Effects of UGN (100 nM) (left) and bradykinin (BK, 1 □M) (right) occur in cerebellar cortex (a, WT = solid line; GC-C KO = dashed line) and cerebral cortex (b). Experiments were performed in 3 animals per group for each brain region. The results are given as mean ± SEM. *-statistical significance difference between WT and GC-C KO mice at p<0.05.

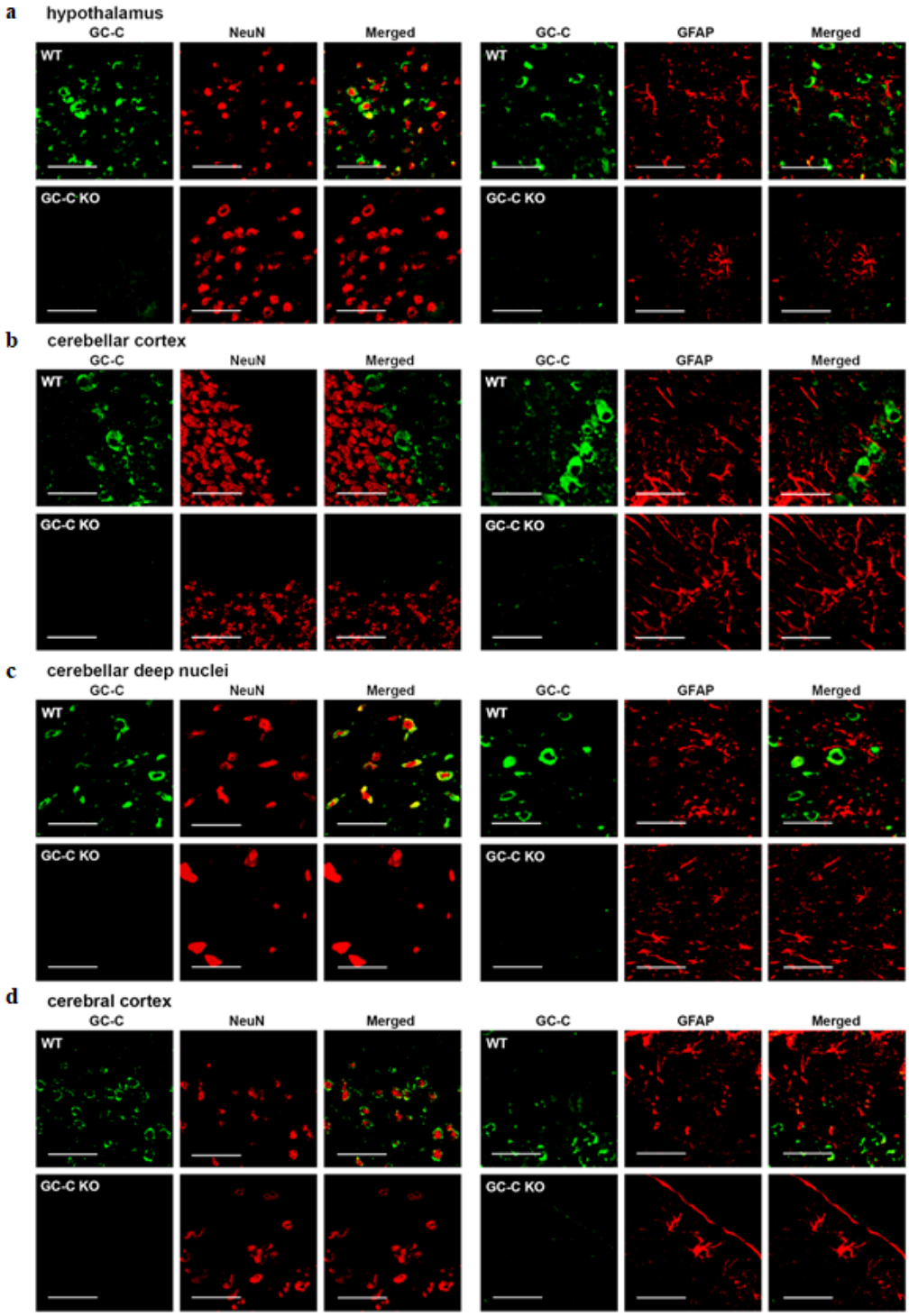

Figure 2

GC-C is expressed in neurons of different brain regions. GC-C (green) co-localized with neuronal marker Neuronal Nuclei marker (NeuN = red, left panel) but not astrocytes marker, Gliar Fibrillary Acidic Protein (GFAP = red, right panel) in (a) hypothalamus, (b) cerebellar cortex, (c) cerebellar deep nuclei and (d) cerebral cortex of WT mice. GC-C knockout (GC-C KO) mice were used as negative control. Bar represents 50 um.

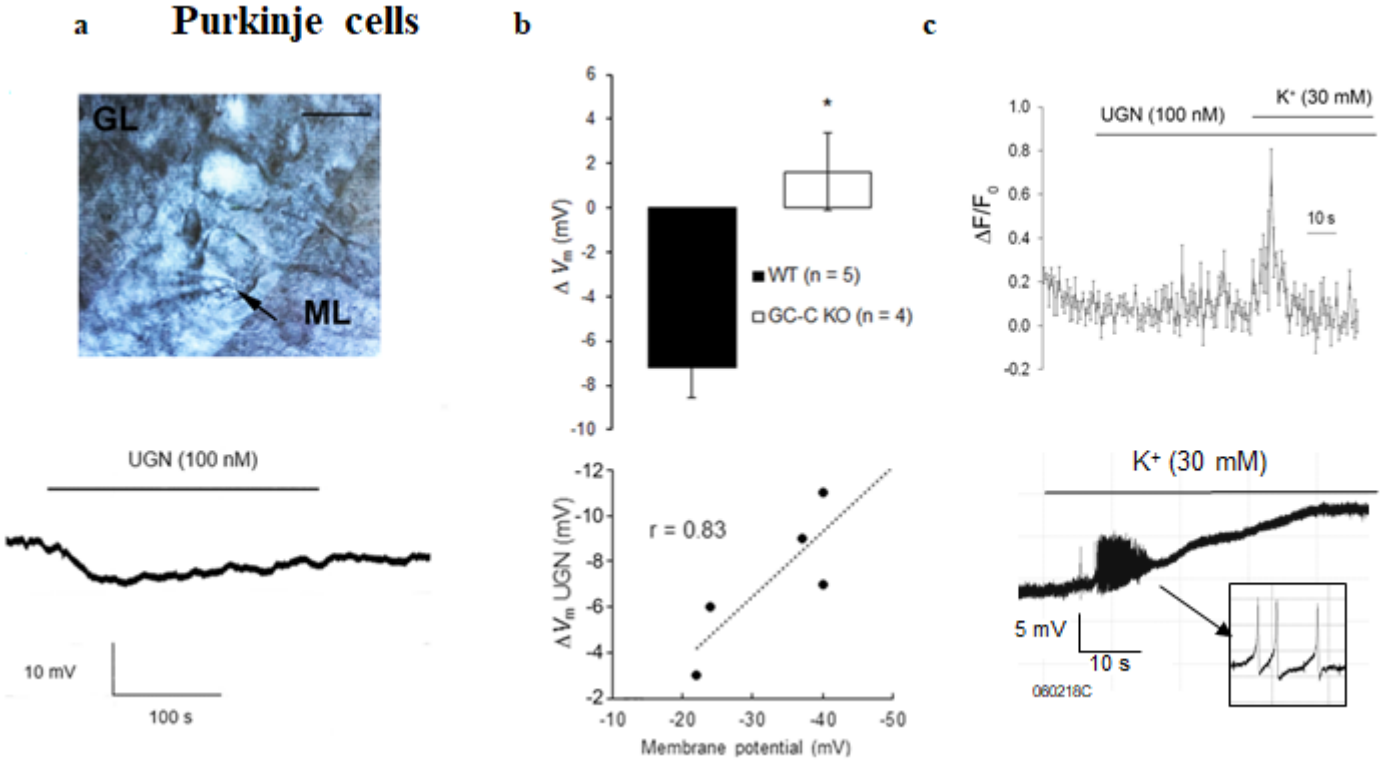

Figure 3

Only uroguanylin GC-C dependent signalling pathway is present in Purkinje cells of cerebellar cortex. Uroguanylin (UGN, 100 nM) in the cerebellum hyperpolarized Purkinje cells (a - upper figure represents DIC scan of cerebellar cortex, arrow pointed in the position where patch clamp pipette is connected to cell membrane of Purkinje cell; ML - molecular layer, GL - granular layer, lower figure - original trace). UGN effects are not present in GC-C KO animals (b, brain slices from WT and GC-C KO animals, n=3 each). Hyperpolarisation effects of UGN were in positive concentration with the membrane potential (b - lower panel). UGN doesn't change intracellular Ca2+concentration of Purkinje cells (c, n = 5, from 3 brain slices of 3 animals). Increased K+ concentrations were used as positive control and increase in Ca2+ concentrations due to hyperkalaemia (Fig. 3c - upper panel) corresponds to occurrence of action potentials (Fig. 3c - lower panel, original trace).The results are given as mean ± SEM. *- $p<0.05$ statistical significance compared to WT mice.

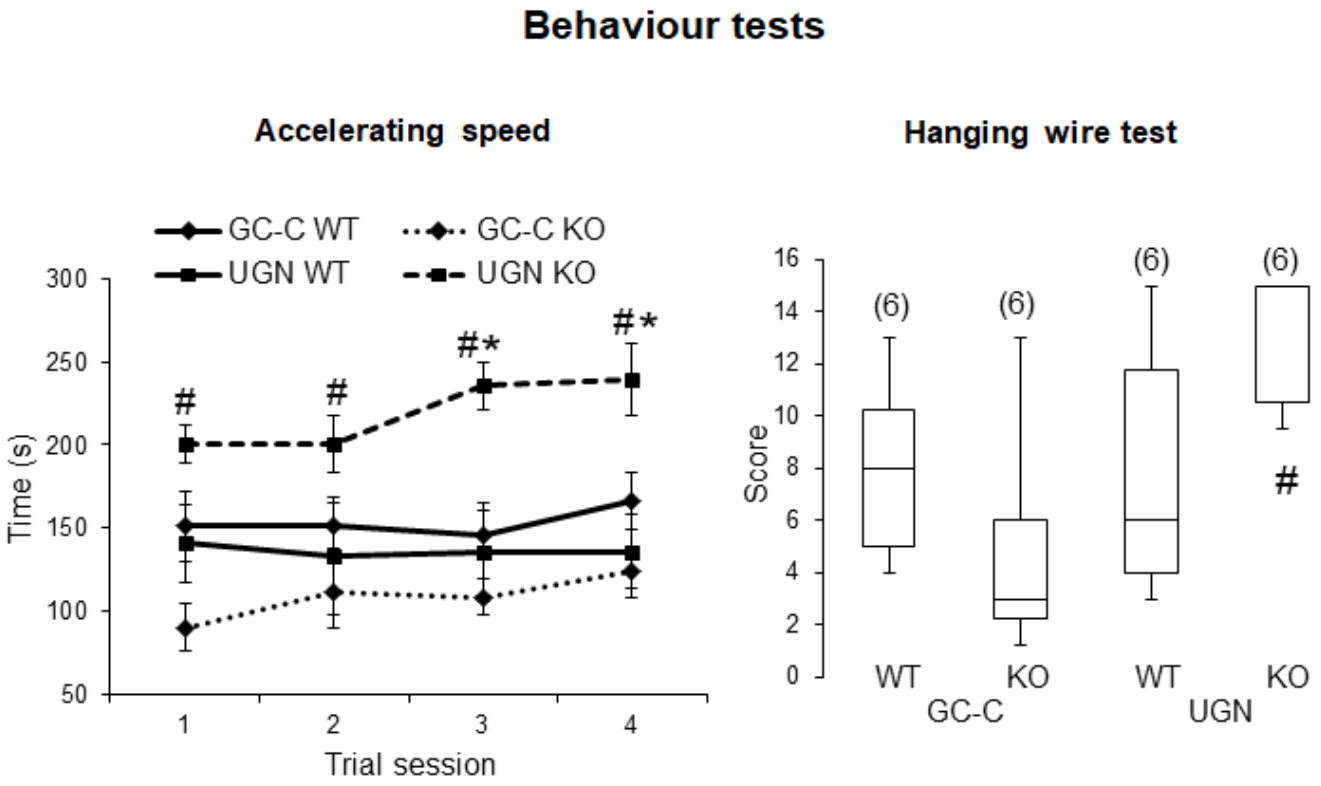

Figure 4

Uroguanylin (UGN) KO mice performed better in behaviour tests compared to their UGN WT littermates and GC-C KO mice. Accelerating speed rota-rod test showed that UGN KO mice stayed on the rod longer than GC-C KO animals. In repeated trials UGN KO performed even better than UGN WT littermates (panel on the left). The results are given as mean ± SEM. *- $p<0.05$ statistical significance compared to WT littermates, #- $p<0.05$ statistical significance compared to GC-C KO mice (ANOVA post hoc Tukey test). In hanging wire test, GC-C KO mice scored significantly fewer points compared to UGN KO mice (panel on the right). The results are given as boxplots displaying median, quartiles and extremes. #- $p<0.05$ statistical significance compared to GC-C KO mice (ANOVA post hoc Tukey test). The numbers of experiments are given in brackets.

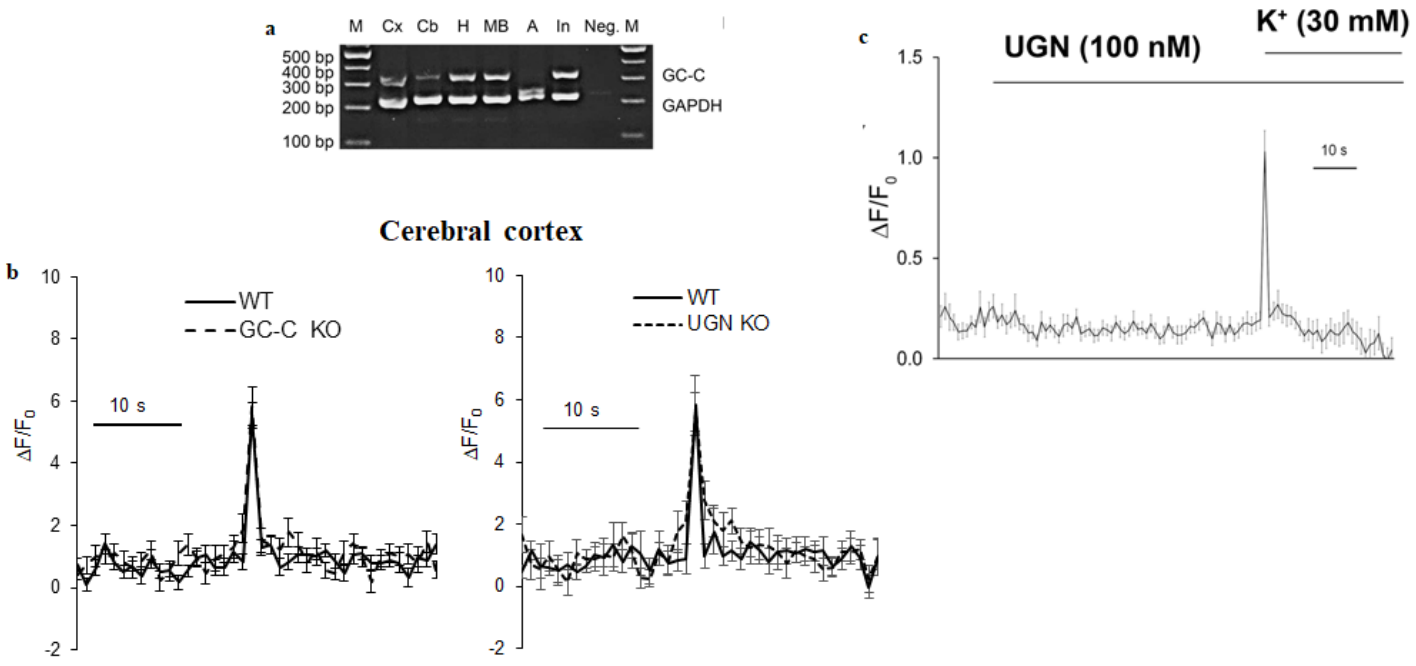

Figure 5

Uroguanylin Ca2+ signalling pathway in cortical astrocytes of brain slices. mRNA of GC-C (341 bp) is expressed in hypothalamus (H), midbrain (MB), cerebral cortex (Cx), and cerebellum (Cb) but not in astrocytes (A) (a). M–marker, In–intestine as positive control, Neg–negative control, GAPDH (235 bp) was used as cDNA control. Ca2+ measurements were performed only in SR101 positive cells (b) of GC-C KO (left, number of animals is 3, number of brain slices is 6, number of cells is 32) and UGN KO (right, number of animals is 3, number of brain slices is 5, number of cells is 14) cerebral cortex and results are compared to their WT littermates (GC-C WT: number of animals is 4, number of brain slices is 6, number of cells is 28; UGN WT: number of animals is 3, number of brain slices is 5, number of cells is 17). In neurons of cerebral cortex of WT animals, there was no effects of UGN on intracellular Ca2+ concentration (number of animals is 4, number of brain slices is 8, number of cells is 43). The hyperkalaemia of 30 mM was used as positive control (c). The results are given as mean ± SEM

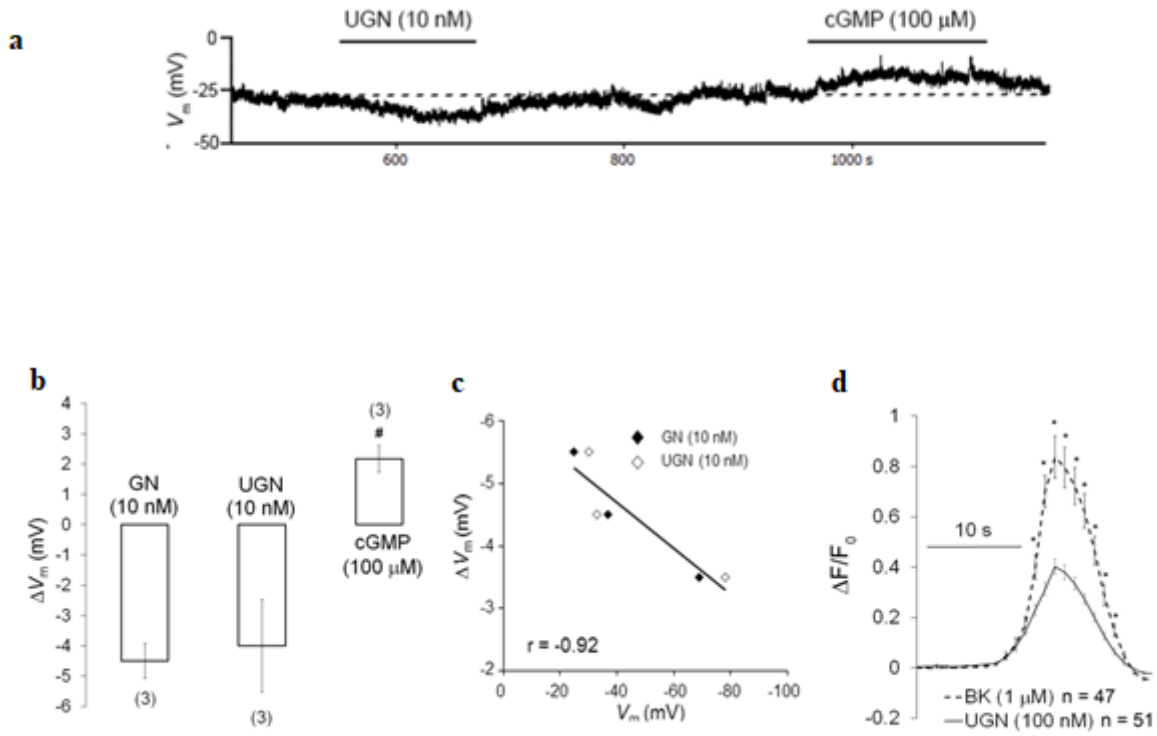

Figure 6

Uroguanylin Ca2+ signalling pathway in astrocytes primary culture. Electrophysiological recording showing an opposite effect of uroguanylin (UGN, 10 nM) compared to membrane permeable cGMP (100 M) on astrocyte membrane potential - original trace. Dashed line represents starting membrane potential (a). Guanylin (GN, 10 nM) and UGN hyperpolarized while membrane permeable cGMP depolarized astrocytes (b). Hyperpolarizations caused by guanylin peptides are in negative correlation to starting membrane potential (c). UGN (100 nM) and bradykinin (BK, 1 M – positive control) increased intracellular Ca2+ concentration (d). The results are given as mean ± SEM. The numbers of experiments is given in brackets. #- statistically significant difference between cGMP effects and effects of guanylin peptides (GN, UGN) at $p<0.05$.* - statistically significant difference between UGN and BK effects at $p<0.05$

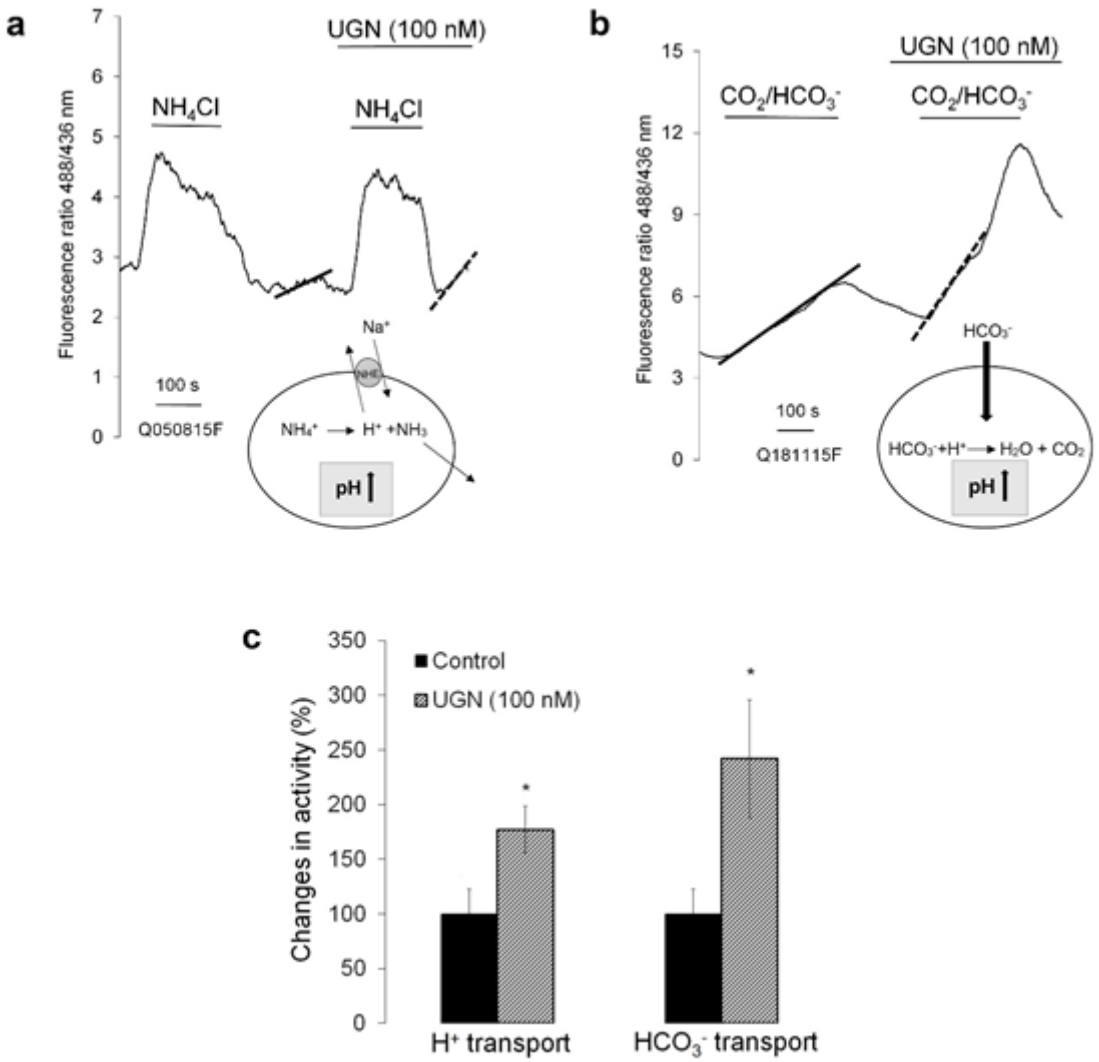

Figure 7

Uroguanylin (UGN) changes the H+ and HCO3- transport in primary culture of astrocytes. UGN increase activity of Na+/H+ exchanger measured by ammonium pulse (a) and HCO3- transport (b) (summarized effects, c). Mechanism of alkalinisation of the cytoplasm due to activation of Na+/H+ exchanger and HCO3- transport is presented in schemes. Mean of the slopes of the control experiments was set to 100%. The results are given as mean ± SEM, n = 3-5, primary culture isolated from 3 new-born animals. *- statistical significance compared to control $p<0.05$. Continuous line - control; dashed line - UGN

Supplementary Files

This is a list of supplementary files associated with this preprint. Click to download.

- Additionalfile1.docx
- Additionalfile2.doc
- ARRIVEchecklist.docx